The Canadian Mineralogist
Vol. 39, pp. 1171-1180 (2001)

CRYSTAL STRUCTURE AND CRYSTAL CHEMISTRY OF LITHIUM-BEARING MUSCOVITE-2M_1

MARIA FRANCA BRIGATTI[§]

Dipartimento di Scienze della Terra, Università di Modena e Reggio Emilia, Via S. Eufemia, 19, I-41100 Modena, Italy

DANIEL E. KILE[§]

U.S. Geological Survey, Denver Federal Center, Denver, Colorado 80225, U.S.A.

MARCO POPPI[§]

Dipartimento di Scienze della Terra, Università di Modena e Reggio Emilia, Via S. Eufemia, 19, I-41100 Modena, Italy

Abstract

Crystal-structure refinements were done on Li-bearing muscovite-2M_1 crystals from microgranite and granitic pegmatite rocks in order to characterize their crystal chemistry and their relationships with muscovite and trioctahedral lithium-containing micas. In addition to the substitution mechanism $^{[6]}Li^{+}\,^{[6]}Al^{3+}_{-1}\,^{[4]}Al^{3+}_{-2}\,^{[4]}Si^{4+}_{2}$, Li-bearing muscovite shows additional substitutions, such as mechanism $^{[6]}Li^{+}\,^{[6]}Fe^{2+}\,^{[6]}Al^{3+}_{-1}\,^{[6]}\square_{-1}$, indicating that the structure deviates from ideal dioctahedral character. Single-crystal X-ray-diffraction data were collected for five crystals in space group *C*2/*c*; the agreement factor, R_{obs}, varies between 0.033 and 0.042. The mean tetrahedral cation–oxygen atom distances range from 1.637 to 1.646 Å and from 1.629 to 1.647 Å for *T*1 and *T*2 sites, respectively. Variation in <*T*–O> distances is associated with the Li^{+} / (Li^{+} + Al^{3+}) ratio, octahedral *M*2 site expansion ($9.30 \le volume_{M2} \le 9.90$ Å^3) and reduction in size of the *M*1 site. Moreover, as the Li^{+} / (Li^{+} + Al^{3+}) ratio increases, the silicate ring becomes less distorted ($5.9 \le \alpha \le 11.4°$), the basal oxygen-atom planes become less corrugated ($0.147 \le \Delta z \le 0.232$ Å), and the interlayer separation narrows (3.337 ≤ interlayer separation ≤ 3.422 Å).

Keywords: lithium, muscovite, crystal structure, crystal chemistry, octahedral occupancy.

Sommaire

Nous avons effectué des affinements de la structure cristalline de la muscovite lithinifère (polytype 2M_1) provenant de microgranite et de pegmatite granitique afin d'en caractériser la cristallochimie et les relations avec la muscovite et les micas trioctaédriques contenant le lithium. En plus du mécanisme de substitution $^{[6]}Li^{+}\,^{[6]}Al^{3+}_{-1}\,^{[4]}Al^{3+}_{-2}\,^{[4]}Si^{4+}_{2}$, la muscovite lithinifère fait preuve de mécanismes additionnels, par exemple $^{[6]}Li^{+}\,^{[6]}Fe^{2+}\,^{[6]}Al^{3+}_{-1}\,^{[6]}\square_{-1}$, indication que la structure s'écarte d'un mica dicotaédrique idéal. Des données de diffraction X ont été prélevées sur cinq cristaux uniques répondant au groupe spatial *C*2/*c*; le facteur de concordance, R_{obs}, varie entre 0.033 et 0.042. La distance moyenne entre le cation à coordinence tétraédrique et l'oxygène varie entre 1.637 et 1.646 Å et entre 1.629 et 1.647 Å pour les sites *T*1 et *T*2, respectivement. La variation en distances <*T*–O> dépend du rapport Li^{+} / (Li^{+} + Al^{3+}), de l'expansion du site octaédrique *M*2 ($9.30 \le volume_{M2} \le 9.90$ Å^3) et de la réduction de la taille du site *M*1. De plus, à mesure que le rapport Li^{+} / (Li^{+} + Al^{3+}) augmente, l'anneau de tétraèdres devient de moins en moins difforme ($5.9 \le \alpha \le 11.4°$), le plan des atomes d'oxygène définissant la base des tétraèdres devient moins ondulant ($0.147 \le \Delta z \le 0.232$ Å), et la séparation inter-feuillet devient moins grande (3.337 ≤ séparation interfoliaire ≤ 3.422 Å).

(Traduit par la Rédaction)

Mots-clés: lithium, muscovite, structure cristalline, cristallochimie, taux d'occupation du site octaédrique.

§ *E-mail addresses*: brigatti@unimo.it, dekile@usgs.gov, marco.poppi@tetrapak.com

INTRODUCTION

Lithium occurs in the octahedral sites of "trisilicic" K-rich micas according to the following exchange-operators: (1) $^{[6]}Li^{+}\ ^{[6]}Al^{3+}{}_{-1}\ ^{[4]}Si^{4+}{}_{2}\ ^{[4]}Al^{3+}{}_{-2}$ and $^{[6]}Li^{+}{}_{3}\ ^{[6]}Al^{3+}{}_{-1}\ ^{[6]}\square_{-2}$ for Fe-free dioctahedral micas, and (2) $^{[6]}Li^{+}\ ^{[6]}Fe^{2+}{}_{-1}\ ^{[4]}Si^{4+}{}_{1}\ ^{[4]}Al^{3+}{}_{-1}$ and $^{[6]}Li^{+}\ ^{[6]}Al^{3+}\ ^{[6]}Fe^{2+}{}_{-2}$ for Fe-bearing trioctahedral micas, although other mechanisms of substitution intermediate between (1) and (2) were reported by Černý & Burt (1984).

Depending on the distribution of cations in the octahedral sites, Li-bearing trioctahedral micas may show complex patterns of long-range order. Some crystals show the common pattern, with a relatively large *trans* site, occupied by monovalent and divalent cations (usually Li^{+}, Fe^{2+} and Mg^{2+}, rarely Mn^{2+}), or vacancies (or both), and with two equivalent smaller *cis* sites preferentially occupied by relatively high-charge cations (typically Al^{3+}, rarely Fe^{3+}) (Takeda & Burnham 1969, Takeda *et al.* 1971, Sartori *et al.* 1973, Sartori 1976, Guggenheim 1981, Swanson & Bailey 1981). In other crystals, trivalent cations are ordered at one of the two *cis* sites (*M*2 or *M*3), whereas Li^{+} and divalent cations occupy the remaining positions (*i.e.*, *M*1 and *M*2, or *M*1 and *M*3), thus producing lower symmetry in the layer, from *C*2/*m* to *C*2 (Guggenheim & Bailey 1977, Guggenheim 1981, Backhaus 1983, Mizota *et al.* 1986, Rieder *et al.* 1996, Brigatti *et al.* 2000).

The mechanism of Li incorporation in the brittle mica bityite-2M_1 $[(Ca_{0.95}Na_{0.02})\ (Li_{0.55}\square_{0.45}Al_{2.04}\ Fe^{3+}{}_{0.01})\ (Al_{1.34}Si_{2.02}Be_{0.64})\ O_{10}\ (OH)_2]$ suggests an octahedral occupancy midway between dioctahedral and trioctahedral (Lin & Guggenheim 1983). The *trans M*1 site is occupied by Li^{+} and vacancies. The two *cis M*2 sites are occupied by Al^{3+} cations. Lin & Guggenheim (1983) attributed this pattern of order to the existence of sheets of dioctahedral (with *M*1 site vacant) and trioctahedral character (with Li-filled *M*1 sites).

Monier & Robert (1986a, b) presented an experimental study of the miscibility gap between trioctahedral and dioctahedral micas in the system K_2O–Li_2O–MgO–FeO–Al_2O_3–SiO_2–H_2O–HF at 600°C, under 2 kbar $P(H_2O)$. The gap between dioctahedral and trioctahedral micas was found to be large in the lithium-free system (Monier & Robert 1986a, Zane & Rizzo 1999), whereas its width decreases progressively with increasing Li content. For Li contents greater than 0.6 atoms per formula unit, a single Li mica phase intermediate between dioctahedral and trioctahedral micas was obtained (Monier & Robert 1986b).

In addition to octahedrally coordinated sites, Li^{+} may substitute for K^{+} in the interlayer. This homovalent exchange-mechanism was suggested by Volfinger & Robert (1979, 1980) and by Robert *et al.* (1983) for synthetic trioctahedral micas. In these micas, Li was found to be located in a pseudo-octahedral cavity defined by the basal oxygen atoms of two tetrahedra located in two adjacent layers.

At present, there are relatively few published studies on lithium-bearing muscovite. We report results of five crystal-structure refinements of muscovite crystals with varying Li contents, and we compare the results with those of previously published crystal-chemical studies on Li-bearing micas.

SAMPLES

Crystals of Li-bearing muscovite were taken from samples of microgranite and granitic pegmatite. Sample 39, from the Fregeneda pegmatite, Salamanca, Spain, is associated with quartz, cassiterite and albite (Roda *et al.* 1995). Sample 2 is from the microgranite at Argemela, Portugal (Charoy & Noronha 1996). Samples 129 and 147 are from the anorogenic Pikes Peak batholith (Colorado). Sample 129 is from a miarolitic cavity in the Redskin Granite near Spruce Grove Campground (Tarryall area, Park County). The muscovite is associated with microcline, fluorite, and smoky quartz (Kile & Foord 1998). That highly evolved pluton is enriched in Li and Be (see Hawley 1969, Hawley & Wobus 1977, Desborough *et al.* 1980) and hosts topaz-bearing pegmatites. Sample 147 is from near Glen Cove (El Paso County) and is associated with microcline and smoky quartz (Kile & Foord 1998). As with the Tarryall area, this locality also involves a highly evolved pluton that contains topaz-bearing pegmatites. The high level of geochemical differentiation of these two Colorado localities is further indicated by the presence of dioctahedral mica within the miarolitic cavities, in contrast to trioctahedral mica that is found elsewhere in the Pikes Peak batholith (Kile & Foord 1998).

EXPERIMENTAL METHODS

Electron-microprobe analysis and normalization of the formula unit

Chemical compositions of single crystals of muscovite (Table 1) were established by energy-dispersion and wavelength-dispersion methods (ARL–SEMQ equipped with Tracor Northern EDS apparatus, operating conditions: accelerating voltage 15 kV, sample current 15 nA, and beam diameter 5 μm). In each sample, several spots were analyzed to check for sample homogeneity. The F content was determined by the method reported by Foley (1989). No evidence of volatilization of F was observed. Analysis and data reduction were performed using the Probe software package of Donovan (1995). Lithium determinations were performed using inductively coupled plasma – atomic emission spectrometry (ICP–AES, Varian Liberty 200). Twenty-five mg of each sample was digested with a mixture of HF (62%) and HNO_3 (38%) in closed Teflon crucibles in a microwave. The OH content was obtained on material from the same concentrate by means of Seiko SSC 5200 thermogravimetric analysis (TG) equipped with a mass

TABLE 1. AVERAGE CHEMICAL COMPOSITION AND CHEMICAL FORMULAE OF LITHIUM-BEARING MUSCOVITE CRYSTALS

	39	2a	2b	147	129
SiO_2 wt.%	45.86	46.43	47.46	46.58	47.20
Al_2O_3	36.29	33.77	32.65	27.33	26.48
TiO_2	0.06	0.01	0.02	0.02	0.10
Fe_2O_3	b.d.t.	b.d.t.	b.d.t.	1.33	1.52
FeO	1.39	2.34	2.38	6.70	5.71
MgO	0.16	0.09	0.10	b.d.t.	0.04
MnO	0.03	0.11	0.12	0.18	0.43
Li_2O	0.11	0.45	0.45	0.99	1.32
Na_2O	0.42	1.11	1.13	0.10	0.11
Rb_2O	0.19	0.50	0.52	0.59	0.35
K_2O	11.05	10.02	10.00	10.85	11.04
H_2O	4.00	3.80	3.82	3.38	3.08
F	0.43	1.36	1.34	1.95	2.61
Sum	99.99	99.99	99.99	100.00	99.99
Structural formulae based on $O_{12-(x+y)}$ OH_x F_y					
$^{[4]}$Si *apfu*	3.072	3.128	3.193	3.242	3.280
$^{[4]}$Al	0.928	0.872	0.807	0.758	0.720
$^{[6]}$Al	1.937	1.810	1.785	1.485	1.449
$^{[6]}$Ti	0.003	....	0.001	0.001	0.005
$^{[6]}Fe^{3+}$	....	....	....	0.073	0.083
$^{[6]}Fe^{2+}$	0.078	0.132	0.133	0.390	0.332
$^{[6]}$Mg	0.016	0.009	0.009	....	0.004
$^{[6]}$Mn	0.002	0.006	0.007	0.010	0.025
$^{[6]}$Li	0.030	0.122	0.122	0.277	0.369
$^{[6]}$Sum	2.066	2.079	2.057	2.236	2.267
$^{[12]}$Na	0.054	0.145	0.147	0.013	0.015
$^{[12]}$Rb	0.008	0.022	0.022	0.026	0.015
$^{[12]}$K	0.944	0.861	0.858	0.963	0.978
OH	1.787	1.707	1.714	1.569	1.427
F	0.091	0.289	0.285	0.429	0.573
O	10.122	10.004	10.001	10.002	10.000

b.d.t.: below detection threshold.

TABLE 2. DETAILS OF THE X-RAY DATA COLLECTION, STRUCTURE REFINEMENT, AND UNIT-CELL PARAMETERS OF LITHIUM-CONTAINING MUSCOVITE CRYSTALS

	N_{obs}	R_{sym} ×100	R_{obs} ×100	a (Å)	b (Å)	c (Å)	β (°)	V (Å^3)
39	1183	2.17	3.51	5.193(1)	9.016(3)	20.114(5)	95.77(2)	937.0
2a	1353	2.65	4.18	5.197(1)	9.019(2)	20.068(3)	95.71(1)	936.0
2b	934	2.77	3.32	5.190(2)	9.022(3)	20.057(4)	95.60(7)	934.7
147	1035	4.73	4.10	5.209(2)	9.038(3)	19.997(5)	95.70(3)	936.8
129	912	3.37	3.53	5.224(1)	9.081(3)	19.952(4)	95.63(2)	941.9

Note: standard deviations are given in parentheses. $R_{sym} = \frac{\sum_{hkl}\sum_{i=1}^{N}|Ihkl_i - Ihkl|}{\sum_{hkl}\sum_{i=1}^{N}Ihkl}$.

spectrometer (ESS, GeneSys Quadstar 422). A sample of about 2–3 mg of powder was heated at a rate of 10°C/min in Ar gas (flow rate 30 mL/min). The ratio of Fe^{2+} to Fe^{3+} was determined following the method reported by Meyrowitz (1970). Chemical compositions reported in Table 1 were obtained by combining the above results. The chemical formula was based on $O_{12-x-y}(OH)_xF_y$.

Collection of X-ray-diffraction data

Several crystals were examined initially by single-crystal precession photographs to determine crystal quality and the polytypes present. Crystals selected for further investigation were mounted onto a Siemens P4P rotating-anode fully automated four-circle diffractometer with graphite-monochromatized Mo$K\alpha$ radiation (λ = 0.71073 Å, 50 kV, 140 mA) equipped with XSCANS software (Siemens 1993). The unit-cell parameters were refined on 40–50 reflections and are reported in Table 2. Intensities for reflections $\pm h, \pm k, + l$ were collected at $2\theta \leq 70.0°$ using the ω scan mode (window width from 2.5 to 4.0°), with scan speeds inversely proportional to intensity, varying from 1 to 5°/minute. The intensity data were then corrected for

TABLE 3. SELECTED BOND-LENGTHS (Å) FROM STRUCTURE REFINEMENT OF LITHIUM-CONTAINING MUSCOVITE CRYSTALS

	39	2a	2b	147	129
Tetrahedron (*T*1)					
*T*1-O11	1.637(2)	1.639(4)	1.634(2)	1.659(3)	1.647(3)
*T*1-O21	1.641(2)	1.650(4)	1.646(2)	1.624(3)	1.649(3)
*T*1-O22	1.647(2)	1.639(4)	1.638(2)	1.639(3)	1.628(3)
*T*1-O31	1.657(2)	1.644(3)	1.637(2)	1.628(3)	1.625(2)
<*T*1-O>	1.646	1.643	1.639	1.638	1.637
Tetrahedron (*T*2)					
*T*2-O11	1.645(2)	1.639(4)	1.626(2)	1.632(3)	1.613(3)
*T*2-O21	1.651(2)	1.645(4)	1.643(2)	1.643(3)	1.637(3)
*T*2-O22	1.642(2)	1.644(4)	1.649(2)	1.639(3)	1.643(3)
*T*2-O32	1.649(2)	1.642(3)	1.638(2)	1.621(3)	1.623(4)
<*T*2-O>	1.647	1.643	1.639	1.634	1.629
Octahedron (*M*2)					
*M*2-O31	1.928(2)	1.954(3)	1.959(2)	1.961(3)	1.993(3)
*M*2-O31'	1.936(2)	1.933(3)	1.939(2)	1.975(3)	1.959(3)
*M*2-O32	1.924(2)	1.927(3)	1.939(2)	1.963(3)	1.961(2)
*M*2-O32'	1.940(2)	1.943(3)	1.950(2)	1.940(3)	1.963(2)
*M*2-O4	1.923(2)	1.931(3)	1.939(2)	1.948(3)	1.962(3)
*M*2-O4'	1.909(2)	1.932(4)	1.937(2)	1.907(3)	1.938(3)
<*M*2-O>	1.927	1.937	1.944	1.949	1.963
Vacant site (*M*1)					
*M*1-O31 (× 2)	2.272(2)	2.243(3)	2.209(2)	2.239(3)	2.227(2)
*M*1-O32 (× 2)	2.277(2)	2.244(3)	2.211(2)	2.246(3)	2.231(2)
*M*1-O4 (× 2)	2.197(2)	2.171(3)	2.151(2)	2.193(2)	2.185(3)
<*M*1-O>	2.249	2.219	2.190	2.226	2.214
Interlayer cation					
A-O11 (× 2)	2.875(2)	2.896(4)	2.916(2)	2.898(3)	3.012(3)
A-O11' (× 2)	3.540(2)	3.475(4)	3.431(3)	3.444(3)	3.308(3)
A-O21 (× 2)	2.868(2)	2.873(4)	2.887(3)	2.936(3)	2.942(3)
A-O21' (× 2)	3.277(2)	3.271(4)	3.265(3)	3.204(3)	3.217(3)
A-O22 (× 2)	2.854(2)	2.862(4)	2.884(2)	2.899(3)	2.966(2)
A-O22' (× 2)	3.298(2)	3.296(4)	3.275(3)	3.243(3)	3.186(2)
A-O4 (× 2)	4.023(2)	4.012(3)	4.011(2)	3.988(3)	3.953(3)
<*A*-O>$_{inner}$	2.866	2.877	2.896	2.911	2.973
<*A*-O>$_{outer}$	3.372	3.347	3.324	3.297	3.237

Note: standard deviations are given in parentheses.

Lorentz-polarization and absorption effects (North *et al.* 1968). The intensities of equivalent reflections were averaged, and the resulting discrepancy factor, R_{sym}, was calculated (Table 2). The structure refinements were performed in the space group *C*2/*c* using a modified version of ORFLS least-squares program (Busing *et al.* 1962) following the same assumptions as adopted by Brigatti *et al.* (1998) for crystals of ferroan and magnesian muscovite. Atom-position parameters from Brigatti *et al.* (1998) were used as initial values for all refinements. Appropriate fully ionized scattering factors were used for octahedral *M* and interlayer *A* cations, whereas half-ionized scattering factors were assumed for oxygen atoms and cations in tetrahedral sites. At the final stage of the refinement, a difference-Fourier electron-density (DED) map was calculated. For all crystals, an electron-density excess in the "vacant" *M*1 site was found on the DED map. Introduction of this partial occupancy in the refinement significantly improved the agreement index (R_{obs}). In the final cycles, anisotropic displacement parameters for *T*, *M*2, and O and isotropic displacement parameters for *M*1 were refined. The final refinement yielded the R_{obs} values reported in Table 2. *M*1 site position was constrained to be isotropic. A final calculated DED map does not reveal a significant excess in electron density above background. In Table 3, we report relevant cation–anion bond lengths, whereas in Table 4, we list selected geometrical parameters obtained from structure refinements. Site populations at *M*1 and *M*2 (Table 5) were determined from the refined structural parameters and from the results of electron-microprobe analyses. Chemical and structural data were treated by a minimization procedure, based on the function labeled "FMINS" in the MATLAB program library (Moler 1992). Details are presented in Brigatti *et al.* (2000). Atom coordinates and equivalent isotropic and anisotropic displacement factors are reported in Table 6, whereas the observed and calculated structure-factors are available from the Depository of Unpublished Data, CISTI, National Research Council, Ottawa, Ontario K1A 0S2, Canada.

TABLE 4. SELECTED PARAMETERS OBTAINED FROM STRUCTURE REFINEMENT OF LITHIUM-BEARING MUSCOVITE

	39	2a	2b	147	129
Parameters describing the tetrahedra					
α (°)	11.4	10.6	9.7	8.7	5.9
Δz (Å)	0.232	0.198	0.172	0.179	0.147
τ_{T1} (°)	110.9	111.2	111.6	111.6	111.6
τ_{T2} (°)	110.9	111.3	111.5	111.9	111.7
TAV_{T1} (°²)	5.43	4.85	6.09	8.24	6.45
TAV_{T2} (°²)	5.48	5.68	6.26	9.54	7.57
$Volume_{T1}$ (Å³)	2.28	2.27	2.25	2.25	2.25
$Volume_{T2}$ (Å³)	2.29	2.27	2.25	2.23	2.21
Parameters describing the octahedra					
ψ_{M1} (°)	62.4	62.1	61.8	61.7	61.5
ψ_{M2} (°)	57.2	57.5	57.8	57.2	57.4
OAV_{M1} (°²)	114.08	105.85	98.52	96.29	90.82
OAV_{M2} (°²)	62.38	53.68	47.80	49.03	43.60
$Volume_{M1}$ (Å³)	14.33	13.83	13.35	14.04	13.86
$Volume_{M2}$ (Å³)	9.30	9.47	9.60	9.67	9.90
Sheet thickness					
Tetrahedral (Å)	2.249	2.252	2.255	2.241	2.238
Octahedral (Å)	2.087	2.081	2.072	2.110	2.114
Interlayer separation (Å)	3.422	3.399	3.399	3.356	3.337
Layer offset (Å)	-0.006	-0.005	-0.005	-0.006	-0.004
Intralayer shift (Å)	0.378	0.373	0.369	0.377	0.374
Overall shift (Å)	-0.389	-0.384	-0.377	-0.381	-0.375

Note: α (tetrahedral rotation angle) = $\sum_{i=1}^{6}\alpha i/6$ where $\alpha_i = |120° - \varphi_i|/2$ and where φ_i is the angle between basal edges of neighboring tetrahedra articulated in the ring. $\Delta z = [Z_{(O_{basal})max} - Z_{(O_{basal})min}]\ [c\sin\beta]$. τ (tetrahedral flattening angle) = $\sum_{i=1}^{3}(O_{basal}-\hat{T}-O_{basal})_i/3$. TAV (tetrahedral angle variance), OAV (octahedral angle variance) = $\sum_{i=1}^{3}(\theta i-109.47)^2/5$, where θ_0 is the ideal bond angle of 109.47° and 90° for a tetrahedron and an octahedron, respectively; n is the coordination number (Robinson *et al.* 1971). ψ (octahedral flattening angle) = $\cos^{-1}$ [octahedral thickness / (2<*M*–O>)] (Donnay *et al.* 1964). For the definition of layer offset, intralayer shift, and overall shift, see Bailey (1984).

Results and Discussion

Exchange mechanisms

The average composition of the five samples of lithium-bearing muscovite (Table 1) is presented in Figures 1 and 2. In trioctahedral micas of the siderophyllite–polylithionite series, the Al^{3+} content in the octahedral sites remains rather constant from siderophyllite to polylithionite, according to the exchange vector $^{[6]}Li^{+}$ $^{[6]}Fe^{2+}_{-1}$ $^{[4]}Si^{4+}_{1}$ $^{[4]}Al^{3+}_{-1}$. In dioctahedral Li-bearing micas, the decrease of $^{[6]}Al^{3+}$ produces a simultaneous

TABLE 5. REFINED AND CALCULATED SITE-OCCUPANCY (*epfu*) FOR CRYSTALS OF LITHIUM-BEARING MUSCOVITE

	39	2a	2b	147	129
***M*1 site**					
Fe	0.01	0.05	0.01	0.19	0.22
Li	0.03	0.02	0.01	0.03	0.02
Mg	0.02	0.01	0.01	—	0.01
vacancy	0.94	0.92	0.96	0.79	0.76
$M1_{XREF}$	0.37	1.56	0.44	4.88	5.86
***M*2 site (× 2)**					
Fe	0.07	0.09	0.13	0.27	0.21
Al	1.94	1.81	1.77	1.48	1.44
Li	—	0.11	0.12	0.25	0.35
$M2_{XREF}$	27.20	26.00	26.20	26.84	25.26
$\Sigma e^-_{(M1\ +\ 2*M2)XREF}$	27.57	27.56	26.64	31.72	31.12
$\Sigma e^-_{(M1\ +\ M2)EPMA}$	27.61	27.59	27.33	32.45	31.51
Interlayer site					
A_{XREF}	18.64	19.02	18.85	19.55	18.64
A_{EPMA}	18.83	18.78	18.71	19.43	18.78

TABLE 6. ATOM COORDINATES AND EQUIVALENT ISOTROPIC AND ANISOTROPIC DISPLACEMENT FACTORS (Å^2) FOR THE CRYSTALS OF LITHIUM-BEARING MUSCOVITE

	x/a	*y/b*	*z/c*	B_{eq}	β_{11}*	β_{22}*	β_{33}*	β_{12}*	β_{13}*	β_{23}*
Sample 39										
O11	0.7513(4)	0.3093(2)	0.1570(1)	1.48(4)	0.0137(7)	0.0051(2)	0.0008(1)	-0.0021(3)	-0.0001(1)	0.0006(1)
O21	0.2496(4)	0.3699(2)	0.1686(1)	1.35(4)	0.0123(7)	0.0048(2)	0.0007(1)	0.0016(3)	0.0002(1)	-0.0001(1)
O22	0.4175(4)	0.0933(2)	0.1679(1)	1.33(4)	0.0189(7)	0.0027(2)	0.0007(1)	0.0006(3)	0.0004(1)	0.0001(1)
O31	0.3840(3)	0.2497(2)	0.0531(1)	1.10(4)	0.0108(6)	0.0039(2)	0.0006(1)	-0.0002(3)	0.0002(1)	0.0001(1)
O32	0.9622(3)	0.4439(2)	0.0534(1)	1.10(4)	0.0081(6)	0.0052(2)	0.0005(1)	0.0008(3)	0.0001(1)	0.0001(1)
O4	0.9558(3)	0.0614(2)	0.0499(1)	0.94(3)	0.0105(6)	0.0016(2)	0.0008(1)	0.0006(3)	0.0006(1)	-0.0001(1)
A	0	0.0994(1)	0.25	1.91(2)	0.0195(3)	0.0060(1)	0.0011(1)	0	0.0004(1)	0
*T*1	0.4518(1)	0.2589(1)	0.13530(3)	0.80(1)	0.0075(2)	0.0024(1)	0.0005(1)	0.0001(1)	0.0001(1)	0.0001(1)
*T*2	0.9651(1)	0.4300(1)	0.13519(3)	0.74(1)	0.0074(2)	0.0020(1)	0.0005(1)	-0.0001(1)	0.0002(1)	0.0001(1)
*M*2	0.2506(1)	0.0834(1)	0.00004(4)	0.84(1)	0.0077(2)	0.0026(1)	0.0005(1)	-0.0005(1)	0.0002(1)	0.0001(1)
*M*1	0.75	0.25	0	2.42(4)						
Sample 2a										
O11	0.7481(7)	0.3125(4)	0.1586(2)	1.40(7)	0.0102(1)	0.0055(4)	0.0009(7)	-0.0018(6)	0.0010(2)	0.0007(1)
O21	0.2467(7)	0.3676(4)	0.1685(2)	1.44(7)	0.0147(1)	0.0052(4)	0.0007(7)	0.0040(6)	0.0005(2)	-0.0002(1)
O22	0.4188(7)	0.0925(4)	0.1676(2)	1.41(7)	0.0203(1)	0.0030(3)	0.0007(1)	0.0001(6)	0.0012(2)	0.0000(1)
O31	0.3905(6)	0.2522(4)	0.0532(1)	0.98(6)	0.0124(1)	0.0031(3)	0.0004(6)	0.0002(5)	0.0007(2)	0.0000(1)
O32	0.9580(6)	0.4405(4)	0.0533(1)	0.92(6)	0.0073(1)	0.0041(4)	0.0005(6)	-0.0001(5)	0.0011(2)	0.0002(2)
O4	0.9548(7)	0.0647(4)	0.0498(2)	1.10(7)	0.0152(1)	0.0032(3)	0.0004(6)	-0.0005(5)	0.0011(2)	-0.0001(1)
A	0	0.0969(2)	0.25	1.76(3)	0.0180(5)	0.0054(2)	0.0010(1)	0	0.0007(1)	0
*T*1	0.4524(2)	0.2573(1)	0.1352(1)	0.65(2)	0.0074(3)	0.0019(1)	0.0004(1)	-0.0005(2)	0.0005(1)	0.0000(1)
*T*2	0.9645(2)	0.4285(1)	0.1351(1)	0.53(2)	0.0060(3)	0.0012(1)	0.0004(1)	-0.0001(2)	0.0008(1)	0.0001(1)
*M*2	0.2526(3)	0.0834(1)	0.00004(6)	0.62(2)	0.0069(4)	0.0018(1)	0.0004(1)	-0.0015(2)	0.0007(1)	0.0001(1)
*M*1	0.75	0.25	0	2.87(7)						
Sample 2b										
O11	0.7459(4)	0.3155(3)	0.1594(1)	1.34(5)	0.0095(7)	0.0052(3)	0.0008(1)	-0.0014(4)	-0.0001(2)	0.0007(1)
O21	0.2459(4)	0.3655(3)	0.1680(1)	1.33(5)	0.0107(8)	0.0052(3)	0.0007(1)	0.0028(4)	0.0005(2)	0.0001(1)
O22	0.4241(4)	0.0922(3)	0.1672(1)	1.33(4)	0.0196(8)	0.0026(2)	0.0007(1)	-0.0003(4)	0.0006(2)	0.0001(1)
O31	0.3966(4)	0.2521(2)	0.0531(1)	0.95(4)	0.0133(7)	0.0026(2)	0.0004(1)	-0.0007(4)	0.0001(1)	-0.0001(1)
O32	0.9540(4)	0.4373(2)	0.0530(1)	0.96(4)	0.0083(7)	0.0039(3)	0.0004(1)	0.0003(3)	0.0003(1)	-0.0001(1)
O4	0.9518(4)	0.0665(2)	0.0496(1)	1.03(4)	0.0129(7)	0.0037(3)	0.003(1)	0.0015(4)	0.0006(1)	-0.0004(1)
A	0	0.0957(1)	0.25	1.63(2)	0.0155(3)	0.0052(1)	0.0010(1)	0	0.0004(1)	0
*T*1	0.4541(1)	0.2571(1)	0.13474(4)	0.51(1)	0.0048(2)	0.0013(1)	0.0004(1)	-0.0003(1)	0.0001(1)	0.0001(1)
*T*2	0.9640(1)	0.4268(1)	0.13478(4)	0.47(1)	0.0037(2)	0.0015(1)	0.0004(1)	-0.0001(1)	0.0003(1)	0.0002(1)
*M*2	0.2527(2)	0.0840(1)	-0.00004(4)	0.56(2)	0.0047(2)	0.0016(1)	0.0004(1)	0.0001(1)	0.0003(1)	-0.0001(1)
*M*1	0.75	0.25	0	2.74 (5)						
Sample 147										
O11	0.7496(5)	0.3173(3)	0.1598(1)	2.15(6)	0.0162(10)	0.0070(3)	0.0016(1)	-0.0005(5)	0.0006(2)	0.0005(1)
O21	0.2415(5)	0.3611(3)	0.1688(1)	2.00(6)	0.0224(11)	0.0040(3)	0.0015(1)	0.0022(4)	0.0015(2)	0.0001(1)
O22	0.4299(5)	0.0941(3)	0.1684(1)	1.93(6)	0.0189(9)	0.0049(3)	0.0014(1)	-0.001(4)	0.0014(2)	0.0001(1)
O31	0.3943(5)	0.2496(3)	0.05431(1)	1.96(6)	0.0148(9)	0.0075(3)	0.0012(1)	-0.0017(5)	0.0010(2)	0.0008(1)
O32	0.9620(4)	0.4378(3)	0.0544(1)	1.62(5)	0.0068(7)	0.0060(3)	0.0014(1)	0.0009(4)	-0.0001(2)	0.0005(1)
O4	0.9524(5)	0.0618(2)	0.0504(1)	1.75(6)	0.0234(10)	0.0020(2)	0.0013(1)	0.0019(4)	0.0009(2)	0.0001(1)
A	0	0.0984(1)	0.25	2.59(3)	0.0218(4)	0.0063(1)	0.0022(1)	0	0.0009(1)	0
*T*1	0.4526(2)	0.2593(1)	0.1357(1)	1.34(2)	0.0102(3)	0.0038(1)	0.0011(1)	-0.0003(2)	0.0007(1)	0.0001(1)
*T*2	0.9663(2)	0.4303(1)	0.1355(1)	1.05(2)	0.0085(3)	0.0014(1)	0.0011(1)	-0.0003(1)	0.0004(1)	0.0002(1)
*M*2	0.2518(2)	0.0825(1)	0.00008(5)	1.41(2)	0.0120(3)	0.0037(1)	0.0011(1)	0.0002(1)	0.0005(1)	0.0002(1)
*M*1	0.75	0.25	0	1.99(5)						
Sample 129										
O11	0.7377(5)	0.3292(3)	0.1611(1)	2.06(6)	0.0151(9)	0.0067(3)	0.0015(1)	-0.0026(4)	0.0002(2)	0.0005(1)
O21	0.2368(5)	0.3598(3)	0.1685(1)	1.89(6)	0.0161(9)	0.0040(3)	0.0017(1)	0.0041(4)	0.0004(2)	-0.0006(1)
O22	0.4446(4)	0.0945(3)	0.1683(1)	1.79(5)	0.0173(8)	0.0036(2)	0.0015(1)	0.0004(4)	0.0007(2)	0.0002(1)
O31	0.3969(5)	0.2527(3)	0.0541(1)	1.80(5)	0.0154(8)	0.0070(3)	0.0009(1)	-0.0010(5)	0.0005(2)	0.0007(1)
O32	0.9567(4)	0.4368(3)	0.0541(1)	1.64(5)	0.0125(8)	0.0049(3)	0.0012(1)	-0.0011(4)	0.0004(2)	0.0009(1)
O4	0.9513(5)	0.0650(3)	0.0515(1)	2.64(6)	0.0327(11)	0.0079(3)	0.0012(1)	-0.0012(5)	0.0010(2)	-0.0001(1)
A	0	0.0950(1)	0.25	2.49(3)	0.0207(4)	0.0069(1)	0.0019(1)	0	0.0005(1)	0
*T*1	0.4546(2)	0.2584(1)	0.13563(4)	1.16(2)	0.0094(3)	0.0030(1)	0.0009(1)	0.0003(2)	0.0003(1)	0.0001(1)
*T*2	0.9640(2)	0.4293(1)	0.13553(4)	1.08(2)	0.0104(3)	0.0014(1)	0.0011(1)	-0.0002(1)	0.0005(1)	0.0001(1)
*M*2	0.2510(2)	0.0826(1)	0.00003(4)	1.15(1)	0.0097(2)	0.0030(1)	0.0009(1)	0.0003(1)	0.0004(1)	0.0002(1)
*M*1	0.75	0.25	0	2.04 (5)						

Notes: * $exp[-(h^2\beta_{11}+...+2hk\beta_{12}+...)]$; standard deviations are given in parentheses. For the *M*1 site, B_{eq} refers to the isotropic displacement parameter. O: anionic sites; *T*: tetrahedral site; *M*: octahedral sites; *A*: interlayer site.

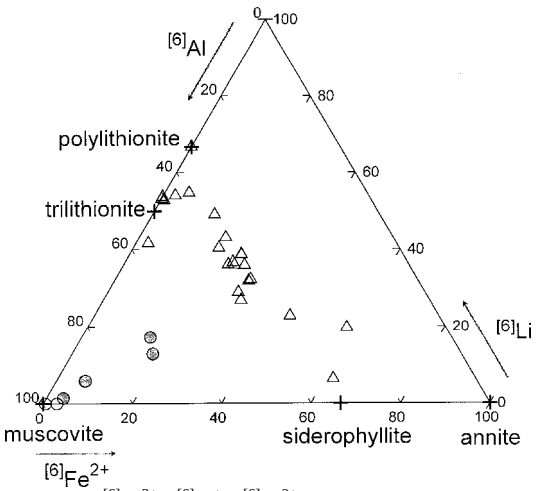

FIG. 1. A $^{[6]}Al^{3+} - {}^{[6]}Li^{+} - {}^{[6]}Fe^{2+}$ diagram (after Rieder *et al.* 1996) illustrating the range in proportion of occupancy of the octahedral sites of Li-bearing muscovite crystals. Filled circles: Li-bearing muscovite crystals from this study. Open symbols represent samples previously described: circles: muscovite (Güven 1971, Guggenheim *et al.* 1987); triangles: trioctahedral Li-bearing micas (Takeda & Burnham 1969, Takeda *et al.* 1971, Sartori 1976, Guggenheim & Bailey 1977, Guggenheim 1981, Backhaus 1983, Hawthorne *et al.* 1999, Brigatti *et al.* 2000). Crosses: end-member compositions.

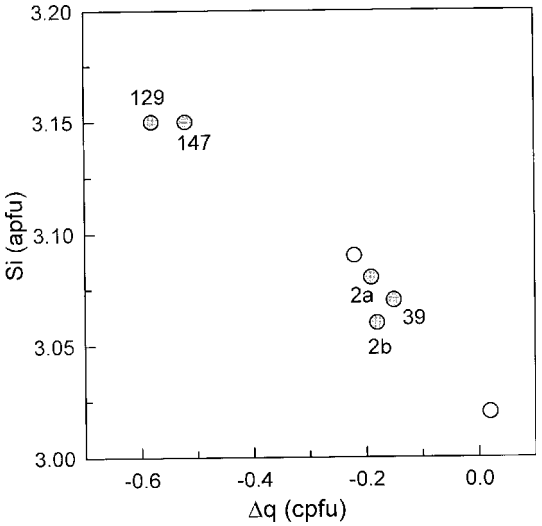

FIG. 2. Variation of $^{[4]}Si$ content with Δq (*i.e.*, the charge variation in the octahedral site with respect to ideal muscovite). Filled circles: Li-bearing muscovite crystals from this study. Open circles represent muscovite crystals from Güven (1971) and Guggenheim *et al.*. (1987).

increase of both $^{[6]}Li^{+}$ and $^{[6]}Fe^{2+}$ content (Fig. 1). Thus, the following exchange-mechanisms may be assumed: (1) $^{[6]}Li^{+}\ {}^{[6]}Fe^{2+}\ {}^{[6]}Al^{3+}_{-1}\ {}^{[6]}\square_{-1}$, which implies a reduction in the dioctahedral character, (2) $^{[6]}Li^{+}\ {}^{[6]}Al^{3+}_{-1}\ {}^{[4]}Si^{4+}_{2}\ {}^{[4]}Al^{3+}_{-2}$, $^{[6]}Fe^{2+}\ {}^{[6]}Al^{3+}_{-1}\ {}^{[4]}Si^{4+}\ {}^{[4]}Al^{3+}_{-1}$ and $^{[6]}Fe^{2+}\ {}^{[6]}\square_{-1}\ {}^{[4]}Al_{2}\ {}^{[4]}Si_{-2}$, which also involve charge balance between tetrahedral and octahedral sites, and (3) the homovalent $^{[12]}Li^{+}\ {}^{[12]}K^{+}_{-1}$ exchange. Figure 2 shows the relationships between Si content and the variation in octahedral charge with respect to ideal muscovite. The relationship further confirms that the cations in the octahedra do not fully balance the octahedral substitution, and thus exchange involving the tetrahedra may need to be considered.

As shown for trioctahedral micas (*e.g.*, Kile & Foord 1998, Brigatti *et al.* 2000), the increase in Li^{+} is associated with an increase in F^{-}. In particular, the proportion in F^{-} is linearly correlated with Li^{+} regardless of the mechanism of incorporation.

S. Guggenheim (pers. commun.) noticed that the rose color displayed by Li-rich muscovite must be related to Mn content, which is a chromophore, and not to Li, which is not a chromophore element. If the polytype is $2M_1$, the mineral is expected to be a "rose muscovite" (another name for Li-bearing muscovite), and if it is either the 1*M*, $2M_2$ or 3*T* polytype, the mineral is expected to be lepidolite. Guggenheim, therefore, suggested that as the Li content is difficult to ascertain, color and polytype appear to be a simple approach to identify the mineral. Data reported in Table 1 and the pink color of the crystals seem to support the above inference.

Crystal-chemical relationships

In the dioctahedral micas examined here, the exchange mechanisms affecting Li incorporation are only approximately similar to those in trioctahedral Li-rich micas and in ferroan and magnesian muscovite. Therefore, the crystal-chemical relationships of Li-containing muscovite are discussed and compared only to the two end-member muscovite crystals reported previously [*i.e.*, the muscovite of Güven (1971) and muscovite from Panasqeira, Portugal of Guggenheim *et al.* (1987)].

The DED maps for all crystals studied indicate a small excess of electron density at the *M*1 position, and thus a partial occupancy of the site. The mean electron count for *M*1 increases from 0.37 to 5.86 e^{-} as the substitution of $^{[6]}Fe^{2+}$ and $^{[6]}Li^{+}$ for $^{[6]}Al^{3+}$ increases. The mean electron count for each *M*2 site is invariably near 13 e^{-}. As the extent of substitutions increase in muscovite, the size of the *M*2 site increases and that of *M*1 decreases. Thus, the difference in volume and in distortion between *M*1 and *M*2 also decreases (Fig. 3). As noted previously (McCauley *et al.* 1973, Lin & Guggenheim 1983), the distortion of an octahedron that shares edges with adjacent octahedra to form a sheet is

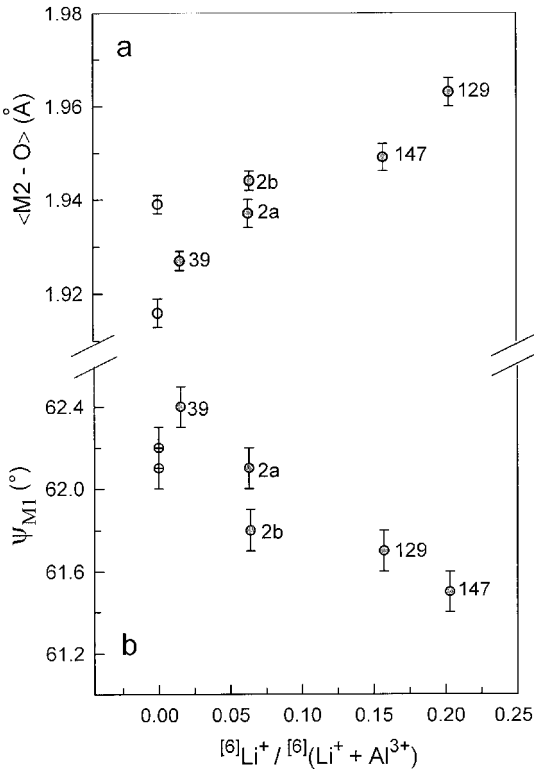

FIG. 3. Compositional dependence of (a) mean (M2 – O) distance with $^{[6]}Li^+ / {}^{[6]}(Li^+ + Al^{3+})$ and (b) of M1 site flattening (ψ_{M1}) with $^{[6]}Li^+ / {}^{[6]}(Li^+ + Al^{3+})$. Symbols and samples as in Figure 2. Error bars represent the estimated standard deviation.

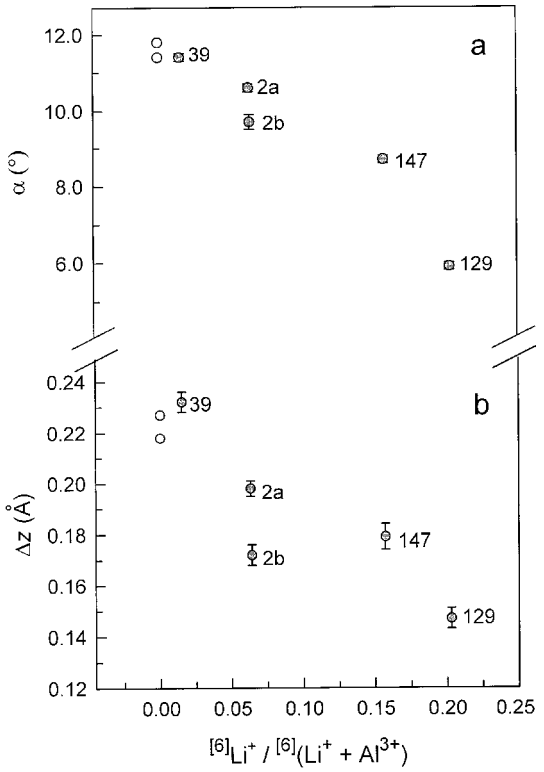

FIG. 4. Compositional dependence of the distortion with $^{[6]}Li^+ / {}^{[6]}(Li^+ + Al^{3+})$. (a) Distortion of the ring of tetrahedra, α, and (b) corrugation of basal plane of oxygen atoms, Δz. Symbols and samples as in Figure 2. Error bars represent the estimated standard deviation.

not a simple function of the size of the cation residing in the octahedron. In fact, in dioctahedral micas, a significant distortion of the vacant site is required to share edges with smaller adjacent octahedra containing cations of high field-strength. Thus, a decrease in the field strength of cations in *M*2, produced by the substitution of Li^+ and Fe^{2+} for Al^{3+}, together with an increase in the field strength of cations at *M*1 owing to partial *M*1 occupancy, further reduce the differences in the two octahedral sites. The smaller differences between the size and distortion of *M*1 and *M*2 have the effect of reducing the corrugation of the surface formed by basal oxygen atoms. Also, the misfit between sheets of tetrahedra and octahedra is reduced, as indicated by the smaller rotation angle of tetrahedra found in the more extensively substituted muscovite crystals from the Pikes Peak batholith (samples 129 and 147) (Fig. 4).

In Li-bearing muscovite, the interlayer separation decreases significantly with increasing incorporation of Li (Fig. 5). This feature may be related to a $^{[12]}Li^+ {}^{[12]}K^+_{-1}$ exchange mechanism. However, the variation in interlayer separation, without assuming the homovalent $^{[12]}Li^+$ for $^{[12]}K^+$ for substitution, may be affected by several factors: (1) the F^- content appears to be directly related to Li^+ substitution, thus the F^- for OH^- substitution at the O4 position precludes electrostatic repulsion between H^+ and the interlayer cation; (2) a large effect on interlayer separation appears to result from the distortion of the ring of tetrahedra from hexagonal to ditrigonal symmetry (Figs. 4a, 5a). A decrease of α results in greater repulsion between the oxygen atoms from two adjacent layers. This effect produces an increase in interlayer separation. In contrast, however, an increase of the size of the interlayer cavity allows the interlayer cation to become embedded more deeply in the ring, thus reducing the interlayer separation. (3) The diminished mismatch between *M*1 and *M*2 produces a shift in the O4 position along [100] toward the interlayer cation. This mechanism accounts for a reduced interlayer separation only if there is F substitution for OH.

The reduced distance between F^- and the interlayer cations allows a greater electrostatic attraction.

There are no significant differences in size ($> 3\sigma$) between *T*1 and *T*2 tetrahedra, and thus they are equivalent with respect to Al and Si occupancy. The surface formed by the basal atoms of oxygen is less corrugated as the substitution affecting octahedral sites proceeds. Thus, the tetrahedral cation increases its distance away from the basal plane of oxygen atoms toward the O3 tetrahedral apex, concomitant with an increase in Li^+ (and Fe^{2+}) for Al^{3+} substitution in the octahedra (Fig. 5b). The displacement of the tetrahedrally coordinated cation seems to be controlled by a substitution involving the *M*2 site and by an increase in tetrahedral charge. Thus, in addition to the exchange mechanism $^{[6]}Al^{3+}{}_{-1}\ ^{[6]}\square_{-1}\ ^{[6]}Li^{+}\ ^{[6]}Fe^{2+}$, our study indicates that exchange mechanisms like $^{[6]}Al^{3+}{}_{-1}\ ^{[6]}Li^{+}\ ^{[4]}Al^{3+}{}_{-2}\ ^{[4]}Si^{4+}{}_{2}$ and $^{[6]}Al^{3+}{}_{-1}\ ^{[6]}(Fe,Mn,Mg)^{2+}\ ^{[4]}Al^{3+}{}_{-1}\ ^{[4]}Si^{4+}$ cannot be excluded.

Acknowledgements

We thank A.E. Blum, J. Flager, and P. Modreski for comments on an early version of this manuscript; S. Guggenheim, R.F. Martin and an anonymous referee provided comments on the final version. The authors are most grateful for samples provided by F. Noronha and E. Roda. This work was supported by Ministero dell'Università e della Ricerca Scientifica of Italy (Project: "Layer silicates: Crystal chemical, structural and petrological aspects") and by Consiglio Nazionale delle Ricerche (CNR) of Italy. Centro Interdipartimentale Grandi Strumenti (CIGS) of the University of Modena e Reggio Emilia is acknowledged for the use of the single-crystal diffractometer. The CNR of Italy is also acknowledged for maintaining the electron microprobe at the Department of Earth Sciences of University of Modena e Reggio Emilia. The use of trade and product names in this paper is for identification purposes only and does not constitute endorsement by the U.S. Geological Survey.

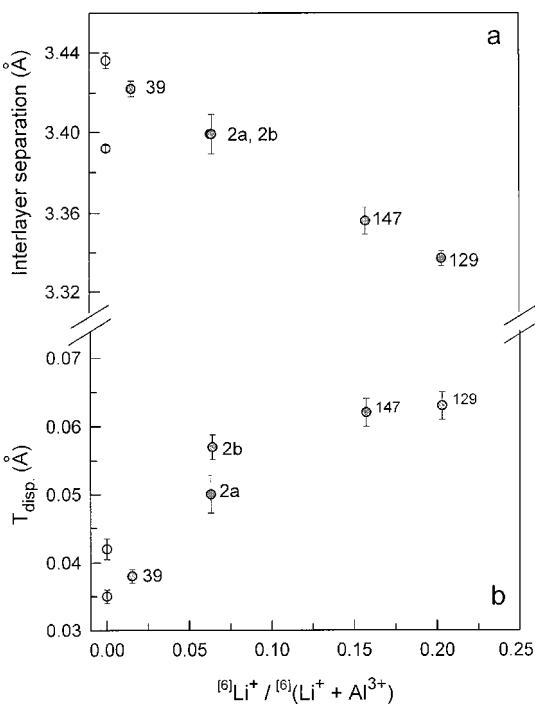

FIG. 5. Relationships between (a) interlayer separation and $^{[6]}Li^+ / {}^{[6]}(Li^+ + Al^{3+})$; (b) shift of the tetrahedrally coordinated cation from the tetrahedron's center of symmetry toward the O3 apex (T_{displ}) *versus* $^{[6]}Li^+ / {}^{[6]}(Li^+ + Al^{3+})$. Symbols and samples as in Figure 2.

References

BACKHAUS, K.O. (1983): Structure refinement of a lepidolite-1*M*. *Crystallogr. Res. Tech.* **18**, 1253-1260.

BAILEY, S.W. (1984): Crystal chemistry of the true micas. *In* Micas (S.W. Bailey, ed.). *Rev. Mineral.* **13**, 13-60.

BRIGATTI, M.F., FRIGIERI, P. & POPPI, L. (1998): Crystal chemistry of Mg-, Fe-bearing muscovites-2M_1. *Am. Mineral.* **83**, 775-785.

_____, LUGLI, C., POPPI, L., FOORD, E.E. & KILE, D.E. (2000): Crystal chemical variations in Li- and Fe-rich micas from the Pikes Peak batholith (central Colorado). *Am. Mineral.* **85**, 1275-1286.

BUSING, W.R., MARTIN, K.O. & LEVY, H.S. (1962): ORFLS, a Fortran Crystallographic Least-Square Program. *U.S. Nat. Tech. Inform. Serv.* **ORNL-TM-305**.

ČERNÝ, P. & BURT, D.M. (1984): Paragenesis, crystallochemical characteristics, and geochemical evolution of micas in granite pegmatites. *In* Micas (S.W. Bailey, ed.). *Rev. Mineral.* **13**, 257-297.

CHAROY, B. & NORONHA, F. (1996): Multistage growth of a rare-element, volatile-rich microgranite at Argemela (Portugal). *J. Petrol.* **37**, 73-94.

DESBOROUGH, G.A., LUDINGTON, S.D. & SHARP, W.N. (1980): Redskin granite: rare-metal-rich Precambrian pluton. Colorado, USA. *Mineral. Mag.* **43**, 959-966.

DONNAY, G., MORIMOTO, N., TAKEDA, H. & DONNAY, J.D.H. (1964): Trioctahedral one-layer micas. I. Crystal structure of a synthetic iron mica. *Acta Crystallogr.* **17**, 1369-1373.

DONOVAN, J.J. (1995): *PROBE: PC-Based Data Acquisition and Processing for Electron Microprobes.* Advanced Microbeam, 4217 King Graves Rd., Vienna, Ohio 44473, U.S.A.

FOLEY, S.F. (1989): Experimental constraints on phlogopite chemistry in lamproites. 1. The effect of water activity and oxygen fugacity. *Eur. J. Mineral.* **1**, 411-426.

GUGGENHEIM, S. (1981): Cation ordering in lepidolite. *Am. Mineral.* **66**, 1221-1232.

_____ & BAILEY, S.W. (1977): The refinement of zinnwaldite-1*M* in subgroup symmetry. *Am. Mineral.* **62**, 1158-1167.

_____, CHANG, Y.-H. & KOSTER VAN GROOS, A.F. (1987): Muscovite dehydroxylation: high-temperature studies. *Am. Mineral.* **72**, 537-550.

GÜVEN, N. (1971): The crystal structures of 2M_1 phengite and 2M_1 muscovite. *Z. Kristallogr.* **134**, 196-212.

HAWLEY, C.C. (1969): Geology and beryllium deposits of the Lake George (or Badger Flats) beryllium area, Park and Jefferson counties, Colorado. *U.S. Geol. Surv., Prof. Pap.* **608-A**.

_____ & WOBUS, R.A. (1977): General geology and petrology of the Precambrian crystalline rocks, Park and Jefferson counties, Colorado. *U.S. Geol. Surv., Prof. Pap.* **608-B**.

HAWTHORNE, F.C., TEERTSTRA, D.K. & ČERNÝ, P. (1999): Crystal-structure refinement of a rubidian cesian phlogopite. *Am. Mineral.* **84**, 778-781.

KILE, D.E. & FOORD, E.E. (1998): Micas from the Pikes Peak batholith and its cogenetic pegmatites, Colorado: optical properties, composition and correlation with pegmatite evolution. *Can. Mineral.* **36**, 463-482.

KNURR, R.A. & BAILEY, S.W. (1986): Refinement of Mn-substituted muscovite and phlogopite. *Clays Clay Minerals* **34**, 7-16.

LIN, JIUN-CHORNG & GUGGENHEIM, S. (1983): The crystal structure of a Li,Be-rich brittle mica: a dioctahedral-trioctahedral intermediate. *Am. Mineral.* **68**, 130-142.

MCCAULEY, J.W., NEWNHAM, R.E. & GIBBS, G.V. (1973): Crystal structure analysis of synthetic fluorophlogopite. *Am. Mineral.* **58**, 249-254.

MEYROWITZ, R. (1970): New semi-microprocedure for determination of ferrous iron in refractory silicate minerals using a sodium metafluoborate decomposition. *Anal. Chem.* **42**, 1110-1113.

MIZOTA, T., KATO, T. & HARADA, K. (1986): The crystal structure of masutomilite, Mn analogue of zinnwaldite. *Mineral. J.* **13**, 13-21.

MOLER, C. (1992): *The Student Edition of MATLAB*. The Math Works Inc., Prentice Hall, Englewood Cliffs, New Jersey.

MONIER, G. & ROBERT, J.-L. (1986a): Muscovite solid solutions in the system K_2O–MgO–FeO–Al_2O_3–SiO_2–H_2O: an experimental study at 2 kbar P_{H2O} and comparison with natural Li-free white micas. *Mineral. Mag.* **50**, 257-266.

_____ & _____ (1986b): Evolution of the miscibility gap between muscovite and biotite solid solutions with increasing lithium content: an experimental study in the system K_2O–Li_2O–MgO–FeO–Al_2O_3–SiO_2–H_2O–HF at 600°C, 2 kbar P_{H2O}: comparison with natural lithium micas. *Mineral. Mag.* **50**, 641-651.

NORTH, A.C.T., PHILLIPS, D.C. & MATHEWS, F.S. (1968): A semi-empirical method of absorption correction. *Acta Crystallogr.* **A24**, 351-359.

RIEDER, M., HYBLER, J., SMRČOK, L. & WEISS, Z. (1996): Refinement of the crystal structure of zinnwaldite 2M_1. *Eur. J. Mineral.* **8**, 1241-1248.

ROBERT, J.-L., VOLFINGER, M., BARRANDON, J.-N. & BASUTÇU, M. (1983): Lithium in the interlayer space of synthetic trioctahedral micas. *Chem. Geol.* **40**, 337-351.

ROBINSON, K., GIBBS, G.V. & RIBBE, P.H. (1971): Quadratic elongation: a quantitative measure of distortion in coordination polyhedra. *Science* **172**, 567-570.

RODA, E., PESQUERA, A. & VELASCO, F. (1995): Micas of the muscovite–lepidolite series from the Fregeneda pegmatites (Salamanca, Spain). *Mineral. Petrol.* **55**, 145-157.

VON ROTHBAUER, R. (1971): Untersuchung eines 2M_1-Muskovits mit Neutronenstrahlen. *Neues Jahrb. Mineral., Monatsh.*, 143-154.

RULE, A.C. & BAILEY, S.W. (1985): Refinement of the crystal structure of phengite-2M_1. *Clays Clay Minerals* **33**, 403-409.

SARTORI, F. (1976): The crystal structure of a 1*M* lepidolite. *Tschermaks Mineral. Petrogr. Mitt.* **23**, 65-75.

_____, FRANZINI, M. & MERLINO, S. (1973): Crystal structure of a 2M_2 lepidolite. *Acta Crystallogr.* **B29**, 573-578.

SIEMENS (1993): XSCANS: *X-ray Single Crystal Analysis System - Technical Reference*. Siemens Instrument. Madison, Wisconsin.

SWANSON, T.H. & BAILEY, S.W. (1981): Redetermination of the lepidolite-2M_1 structure. *Clays Clay Minerals* **29**, 81-90.

TAKEDA, H. & BURNHAM, C.W. (1969): Fluor-polylithionite: a lithium mica with nearly hexagonal $(Si_2O_5)^{2-}$ ring. *Mineral. J.* **6**, 102-109.

_____, HAGA, N. & SADANAGA, R. (1971): Structural investigation of a polymorphic transition between 2M_2-, 1*M*-lepidolite and 2M_1-muscovite. *Mineral. J.* **6**, 203-215.

VOLFINGER, M. & ROBERT, J.-L. (1979): Le lithium dans une phlogopite de synthèse. *Bull. Minéral.* **102**, 26-32.

_____ & _____ (1980): Structural control of the distribution of trace elements between silicates and hydrothermal solutions. *Geochim. Cosmochim. Acta* **44**, 1455-1461.

ZANE, A & RIZZO, G. (1999): The compositional space of muscovite in granitic rocks. *Can. Mineral.* **37**, 1229-1238.

Received March 18, 2001, revised manuscript accepted June 29, 2001.